First-principles experimental observation of coherent hole burnings in atomic rubidium vapor

Xiao-Gang Wei,[1,2] Jin-Hui Wu,[1,2] Hai-Hua Wang,[1,2] Ang Li,[1,2] Zhi-Hui Kang,[1,2] Yun Jiang,[1,2] and Jin-Yue Gao[1,2,3,*]

[1]*College of Physics, Jilin University, Changchun 130023, People's Republic of China*

[2]*Key Laboratory of Coherent Light and Atomic and Molecular Spectroscopy of Ministry of Education, Jilin University, Changchun, People's Republic of China*

[3]*CCAST (World Laboratory), P.O. Box 8370, Beijing 100080, People's Republic of China*

(Received 9 May 2006; published 20 December 2006)

We demonstrate in experiment that the simultaneous use of two laser fields, a saturating and a coupling field, allows us to observe three or four coherent hole burnings with controllable widths, depths, and positions in a single Doppler absorption profile. Appropriate theoretical simulations and analysis show that these correlated coherent hole burnings result from the combination of strong saturating excitation and dynamically induced quantum coherence.

DOI: 10.1103/PhysRevA.74.063820 PACS number(s): 42.50.Gy, 42.50.Hz, 42.62.Fi

I. INTRODUCTION

Optical hole burning is the phenomenon where a saturating field burns a hole into the population distribution at a certain level of an inhomogeneous medium, which is usually called the Bennet hole or Lamb hole when reflected in the absorption spectrum of a probe field [1,2]. So far the spectral hole-burning phenomenon has attracted a great of research interest due to its potential uses in high-resolution spectroscopy, optical information storage, and laser frequency stabilization [3–6]. On the other hand, electromagnetically induced transparency (EIT) [7,8], which utilizes quantum coherence generated by a coupling field to make an otherwise opaque medium transparent to a resonant probe field in a narrow spectral window, has become another research focus since the early 1990s. It was shown that EIT may lead to applications in laser physics, nonlinear optics, and quantum-information science [9–12].

Considering both EIT and hole burning can result in absorption reduction in a narrow spectral range, Dong and Gao first proposed in 2000 the interesting coherent hole-burning (CHB) theory, which allows for the simultaneous observation of an EIT window and four hole burnings at most when two laser beams (one saturating and one coupling) drive a Doppler-broadened atomic medium in the ladder configuration [13]. Later, we extended the CHB theory into a Λ-type Doppler-broadened atomic system where CHBs are much clearer due to the matched transition wavelengths and thus suitable for experimental observation [14].

In this paper, we report the experimental observation of CHBs using ^{87}Rb atomic vapor as the inhomogeneous medium. Depending on the propagation directions of the saturating and coupling beams, we have observed three or four clear CHBs with controllable depths, widths, and positions. Our experimental results are shown to be in good agreement with corresponding theoretical simulations in the bare-state representation. In addition, we have further clarified the underlying physics of CHBs in the dressed-state representation. We note that, for potential applications in optical information processing, the hole-burning storage technique must overcome either its slow writing (recovery) time or limited persistent storage time, and the CHB phenomenon may be quite useful and valuable if suitable solid materials with fast decay processes can be found.

II. THEORETICAL ANALYSIS

We consider a three-level Λ-type atomic system and show the relevant hyperfine levels of the ^{87}Rb $D1$ line in Fig. 1. The hyperfine level $F'=2$ of the $5P_{1/2}$ state serves as the excited level $|3\rangle$ while the hyperfine levels $F=1$ and 2 of the $5S_{1/2}$ state serve as the ground levels $|1\rangle$ and $|2\rangle$, respectively. Levels $|2\rangle$ and $|3\rangle$ are coupled by an intense laser of wavelength 794.983 nm (the coupling field with frequency ω_c and Rabi frequency Ω_c). A weak laser of wavelength 794.969 nm (the probe field with frequency ω_p and Rabi frequency Ω_p) detects the absorption on transition $|1\rangle \leftrightarrow |3\rangle$. An intermediate laser of wavelength 794.969 nm, which acts on the same transition as the probe field, is used as the saturating field with frequency ω_s and Rabi frequency Ω_s. $\Delta_c=\omega_{32}-\omega_c$, $\Delta_s=\omega_{31}-\omega_s$, and $\Delta_p=\omega_{31}-\omega_p$ are the detunings of the three coherent fields, respectively. Γ_{31} and Γ_{32}, respectively, de-

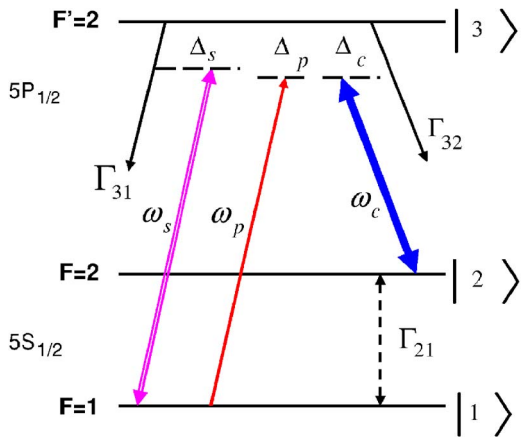

FIG. 1. (Color online) Energy level diagram of the $D1$ line for atomic ^{87}Rb driven by three linearly polarized coherent lasers: a probe, a saturating, and a coupling field.

*Electronic address: jygao@mail.jlu.edu.cn

note the spontaneous decay rates from level $|3\rangle$ to levels $|1\rangle$ and $|2\rangle$, which are both about 6 MHz here. Γ_{21} designates the population transfer rate between levels $|1\rangle$ and $|2\rangle$ due to atomic collisions, and is of the order of kilohertz at room temperature.

In the bare-state representation, we can easily perform full numerical simulations of the probe absorption for our considered ^{87}Rb atomic system [15]. In order to understand how CHBs are generated, however, we have to resort to the dressed-state representation. In the limit of $\Omega_c \gg \Omega_s$, Γ_{31}, $\Gamma_{32} \gg \Omega_p$, we can imagine that level $|3\rangle$ is split into dressed sublevels $|3+\rangle$ and $|3-\rangle$ with $\Delta_\pm = (\Delta_c' \pm \sqrt{\Delta_c'^2 + 4\Omega_c^2})/2$ being their eigenvalues. Here we have included the atomic Doppler effect so that $\Delta_c' = \Delta_c + \eta_c(v/c)\omega_c$, $\Delta_s' = \Delta_s + \eta_s(v/c)\omega_s$, and $\Delta_p' = \Delta_p + (v/c)\omega_p$. $\eta_c = \pm 1$ ($\eta_s = \pm 1$) denotes that the coupling (saturating) field propagates in the same or opposite direction as the probe field. For certain atoms having definite velocities v, if they simultaneously interact with the probe and saturating fields by resonant absorption, CHBs are expected to appear in the probe absorption spectrum due to population depletion. This can be realized in the following ways.

(i) The probe and saturating fields are simultaneously resonant with the dressed transition $|3+\rangle \leftrightarrow |1\rangle$, i.e., $\Delta_p' = \Delta_s' = \Delta_+$.

(ii) The probe (saturating) field is resonant with the dressed transition $|3+\rangle \leftrightarrow |1\rangle (|3-\rangle \leftrightarrow |1\rangle)$, i.e., $\Delta_p' = \Delta_+$ and $\Delta_s' = \Delta_-$.

(iii) The probe and saturating fields are simultaneously resonant with the dressed transition $|3-\rangle \leftrightarrow |1\rangle$, i.e., $\Delta_p' = \Delta_s' = \Delta_-$.

(iv) The probe (saturating) field is resonant with the dressed transition $|3-\rangle \leftrightarrow |1\rangle$ ($|3+\rangle \leftrightarrow |1\rangle$), i.e., $\Delta_p' = \Delta_-$ and $\Delta_s' = \Delta_+$.

In fact, these four resonant conditions can be generalized into the following two equations with v and Δ_p being their variables:

$$\Omega_c^2 = \left(\Delta_s + \eta_s \frac{v}{c}\omega_s\right)\left(\Delta_s + \eta_s \frac{v}{c}\omega_s - \Delta_c - \eta_c \frac{v}{c}\omega_c\right), \quad (1)$$

$$\Omega_c^2 = \left(\Delta_p + \frac{v}{c}\omega_p\right)\left(\Delta_p + \frac{v}{c}\omega_p - \Delta_c - \eta_c \frac{v}{c}\omega_c\right). \quad (2)$$

In the case of the $D1$ line for ^{87}Rb, ω_c is approximately equal to ω_s and ω_p. Thus when $\eta_c = -\eta_s = 1$ ($\eta_c = -\eta_s = -1$), we can obtain from the first equation that $v_{1,2} = [\eta_s(\Delta_c - 3\Delta_s) \pm \sqrt{(\Delta_s + \Delta_c)^2 + 8\Omega_c^2}]c/4\omega_s$ corresponding to the saturating field being resonant with $|3\mp\rangle \leftrightarrow |1\rangle$ ($|3\pm\rangle \leftrightarrow |1\rangle$). This means that two groups, but not a single group, of atoms at level $|1\rangle$ can be excited to saturation due to the presence of the coupling field. With either v_1 or v_2 used in the second equation, we can easily get two different solutions for Δ_p. It is then clear that four CHBs in total could be observed if no degeneracy occurs, which is true for the case of $\eta_c = -\eta_s = 1$. When $\eta_c = -\eta_s = -1$, however, there will exist only three CHBs in the probe absorption spectrum because the two central ones are always located at the same position of $\Delta_p = \Delta_s$.

TABLE I. CHB positions (Δ_p) for the case of $\Delta_c = \Delta_s = 0$.

v_s	$\eta_c = -\eta_s = 1$		$\eta_c = -\eta_s = -1$	
	$\Delta_p' = \Delta_+$	$\Delta_p' = \Delta_-$	$\Delta_p' = \Delta_+$	$\Delta_p' = \Delta_-$
$c\Omega_c/(\sqrt{2}\omega_s)$[a]	$\Omega_c/\sqrt{2}$	$-\sqrt{2}\Omega_c$	0	$-3\Omega_c/\sqrt{2}$
$-c\Omega_c/(\sqrt{2}\omega_s)$[b]	$\sqrt{2}\Omega_c$	$-\Omega_c/\sqrt{2}$	$3\Omega_c/\sqrt{2}$	0

[a]Designates $|3\mp\rangle \leftrightarrow |1\rangle$ for $\eta_c = -\eta_s = \pm 1$.
[b]Designates $|3\pm\rangle \leftrightarrow |1\rangle$ for $\eta_c = -\eta_s = \pm 1$.

Detailed information about CHB positions is illustrated in Table I for $\eta_c = -\eta_s = \pm 1$ and $\Delta_s = \Delta_c = 0$.

III. EXPERIMENTAL SETUP AND RESULTS

The experimental arrangement is illustrated in Fig. 2. The ^{87}Rb atomic vapor contained in a 3-cm-long cylindrical cell is heated to the temperature of about 325 K. The probe beam with linewidth of about 4 MHz is provided by an extended cavity diode laser (DL100) and attenuated to less than 1 μW by a Nd filter before it enters the atomic cell. Two Ti:sapphire lasers (Coherent 899 ring laser) with linewidth of about 500 kHz, Ti:sapphire 1 and Ti:Sapphire 2, are used to provide the coupling and saturating beams, respectively. The coupling and saturating beams are orthogonal in polarization and counterpropagate through the atomic cell with the help of a $\lambda/2$ wave plate as well as a pair of polarization beam splitters. The probe beam, with its polarization parallel to the saturating beam, copropagates with the coupling beam at a small angle of 0.01 rad. The probe beam is always well contained by the other two collinear beams inside the atomic cell, which permits all probed atoms to be coherently prepared. A pinhole is placed in front of the ECDL to block the saturating beam and thus protect the ECDL against feedback. A photodiode is used to detect the absorption spectrum of the probe beam passing through the atomic cell.

The experimental results obtained with such an experimental arrangement are shown in Fig. 3. With the coupling beam on but the saturating beam off, we can observe an EIT window with the contrast of about 80% in the probe absorption spectrum [the upper curve in Fig. 3(a)]. Here the parameter of contrast is defined as the ratio of the EIT depth to the height of the EIT shoulders. The EIT width is about 60 MHz, which is mainly determined by the Rabi frequency of the

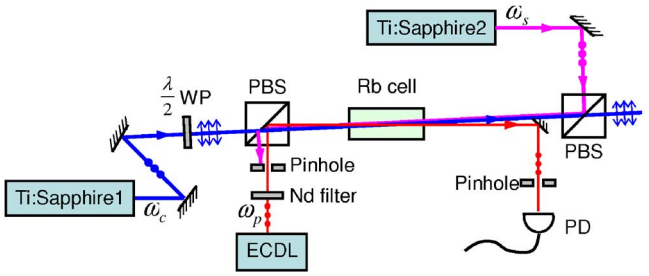

FIG. 2. (Color online) Schematic diagram of the experimental setup. ECDL, external cavity diode laser; $\lambda/2$ WP, half wave plate; PBS, polarization beam splitter; PD, photodiode detector.

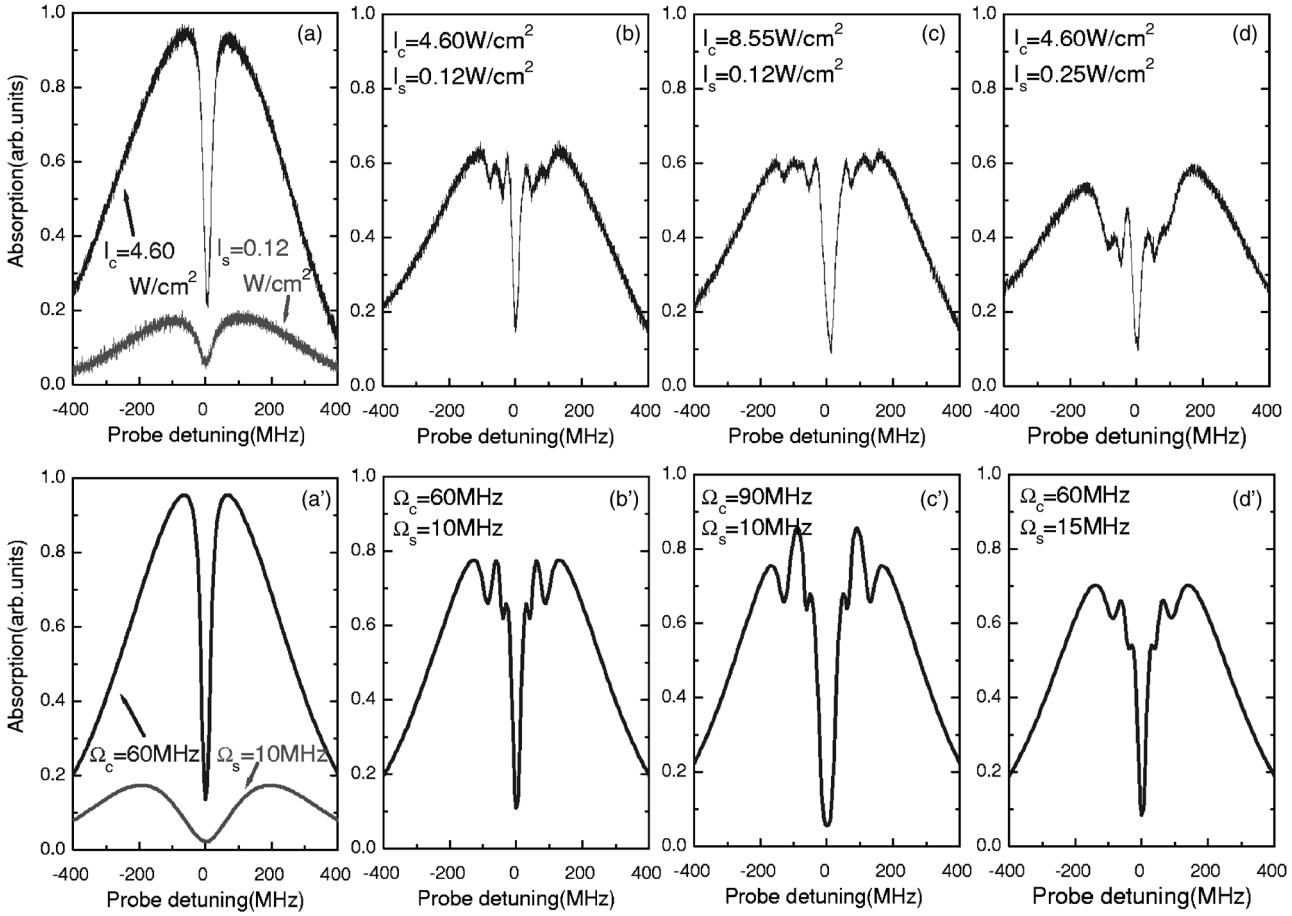

FIG. 3. Experimental results (a)–(d) and corresponding theoretical simulations (a')—(d') for the probe beam copropagating with the saturating beam while counterpropagating with the coupling beam. Parameters used in the theoretical simulations are $\Gamma_{31}=\Gamma_{32}=6$ MHz, $\Gamma_{21}=10$ kHz, and $\Delta_c=\Delta_s=0$ MHz. Here 1 W/cm^2 of the power density for both the coupling and saturating fields corresponds to an effective Rabi frequency of 30.3 MHz.

coupling field. Blocking the coupling beam and then turning on the saturating beam, we can see a conventional hole burning in the probe absorption spectrum [the lower curve in Fig. 3(a)]. With both coupling and saturating beams on, we find that the EIT window becomes a little deeper than before with its position unchanged. More importantly, we can see four CHBs, symmetrically located two at each side of the EIT window. In Fig. 3(b), the positions of these four CHBs are approximately $\Delta_p=\pm 44$ MHz and $\Delta_p=\pm 84$ MHz, which is in good agreement with the theoretical analysis shown in Table I. If we increase the intensity of the coupling field only, we can see from Fig. 3(c) that the EIT window becomes much deeper and wider as expected. Simultaneously, distances between adjacent CHBs become larger with their locations being approximately $\Delta_p=\pm 65$ MHz and $\Delta_p=\pm 135$ MHz due to the much better-detached dressed levels $|3+\rangle$ and $|3-\rangle$. Instead, if we increase the saturating intensity while keep the coupling intensity unchanged, we find from Fig. 3(d) that the four CHBs are still located at the same positions as in Fig. 3(b) because their positions are independent of Ω_s in the limit of $\Omega_c \gg \Omega_s$. Note that the whole absorption curve becomes lower due to the much stronger saturation effect. Clearly, CHBs can be easily controlled by modulating the strengths of both coupling and saturating beams. Figures 3(a)–3(d) present the theoretical simulations of Figs. 3(a)–3(d) using the same approach as in Ref. [14] but with all laser linewidths included.

By simply exchanging the positions of the ECDL (together with the Nd filter) and the photodiode, we have a new experimental arrangement where the coupling (saturating) beam counterpropagates (copropagates) with the probe beam [16]. Corresponding experimental results are shown in Fig. 4. The upper curve in Fig. 4(a) shows the absorption spectrum with only the coupling beam on, where no EIT window exists because the Doppler frequency shifts for coupling and probe beams can not cancel each other. The lower curve, where there exists a conventional hole burning, corresponds to the case of only the saturating beam on. With both coupling and saturating beams on, we can observe instead three CHBs with the central one being much deeper than the other two due to degeneracy [17]. This deep and narrow CHB, which does not result from quantum coherence or EIT, provides us a different way to obtain slow-light propagation with negligible loss. In Fig. 4(b), we estimate the coupling (saturating) beam to have $\Delta_c=-50$ MHz ($\Delta_s=0$) and find that the central CHB is located at $\Delta_p=0$, with the other two at $\Delta_p=-100$ and 75 MHz. This is consistent with the above theoretical analysis, which predicts that CHBs should be,

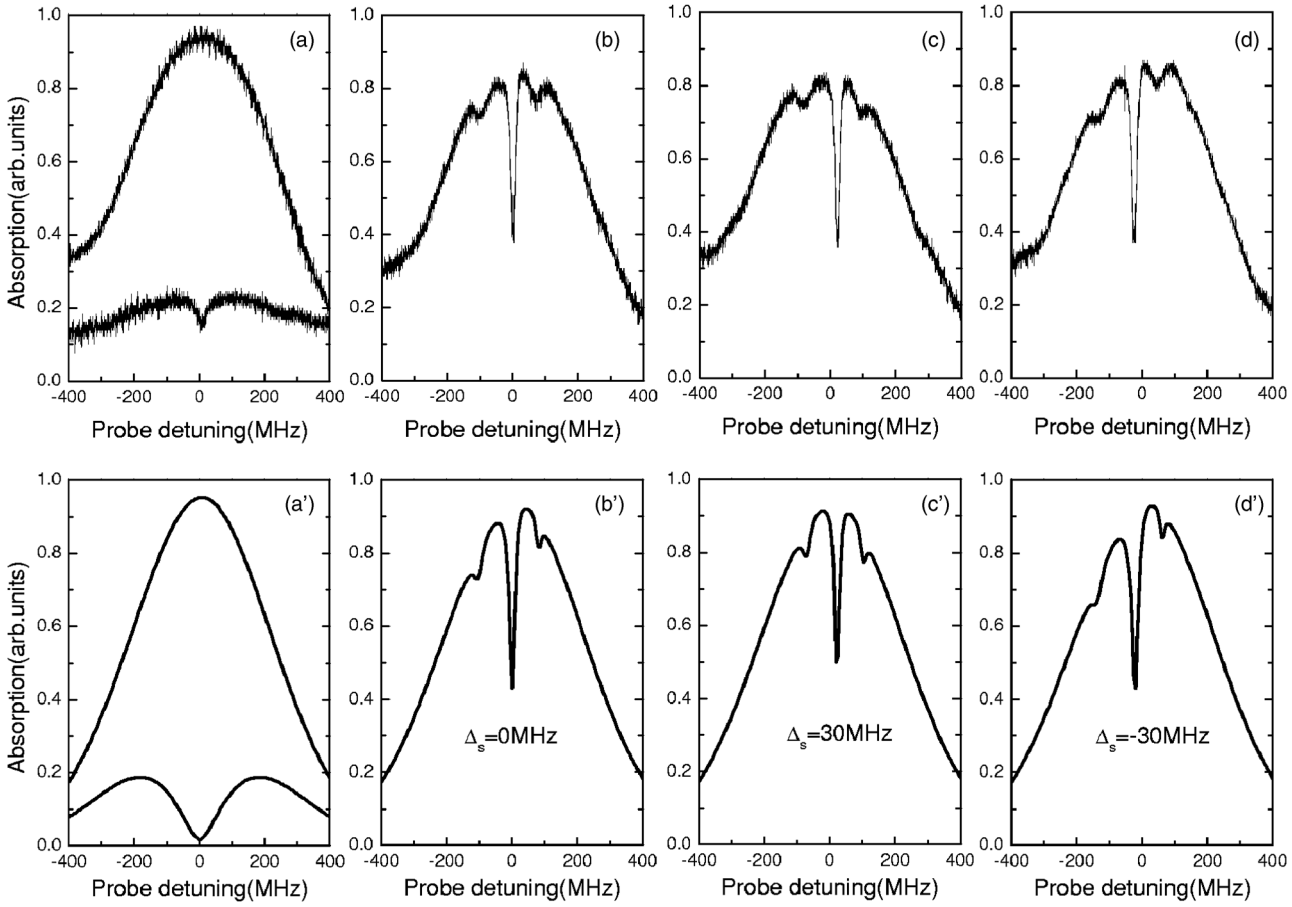

FIG. 4. Experimental results (a)–(d) and theoretical simulations (a')—(d') for the coupling beam counterpropagating and the saturating beam copropagating with the probe beam. Corresponding theoretical and experimental parameters are $\Gamma_{31}=\Gamma_{32}=6$ MHz, $\Gamma_{21}=10$ kHz, $\Omega_c=40$ MHz, $\Omega_s=4$ MHz, $I_c=19.1$ W/cm^2 corresponding to an effective Rabi frequency of about 45 MHz, and $I_s=0.04$ W/cm^2 corresponding to an effective Rabi frequency of 6 MHz.

respectively, located at $\Delta_p=\Delta_s$ and $\Delta_p=[\Delta_c+5\Delta_s\pm3\sqrt{(\Delta_c+\Delta_s)^2+8\Omega_c^2}]/4$. Figures 4(c) and 4(d) further show experimental results for the cases of $\Delta_s=\pm30$ MHz and $\Delta_c=-50$ MHz, where the central CHB moves to $\Delta_p=\pm30$ MHz and the sideward CHBs are asymmetric both in position and in depth. So we also can effectively control CHBs by modulating detunings of both coupling and saturating beams. Figures 4(a)–4(d) are the theoretical simulations of Figs. 4(a)–4(d) with all laser linewidths included.

We now discuss the potential applications of CHB in optical information storage and processing. Via photochemical or photoionization reactions, persistent spectral holes could be burned into organic molecules doped in polymer matrices or rare-earth ions doped in crystalline hosts [18,19]. Persistent spectral hole burnings (PSHBs) constitute a good memory mechanism used for numerous proposed applications, such as optical data storage, optical data processing, spectral-spatial correlation, and temporal pattern recognition [5]. Different kinds of PSHB materials at low temperature have been studied, while those at room temperature are being pursued for the purpose of practical applications. If we can extend the CHB technique from the atomic vapor showing slow decay time and transient spectral hole-burning properties into solid materials exhibiting fast decay time and PSHB properties, PSHB will become much more controllable in width and depth, leading to various more fascinating applications. In particular, the density of stored optical data will be improved three or four times in a given inhomogeneous spectral line. On the other hand, one can store and retrieve quantum information carried by weak optical pulses in EIT media by smoothly turning on or off strong coupling fields [11,12]. This stored quantum information can be processed via greatly enhanced nonlinear optical interactions in EIT media [9]. Noting that CHB arises from EIT and also depends on quantum coherence, we thus infer that quantum information carried by weak optical pulses may be stored, retrieved, and processed in CHB media by similar or extended techniques.

IV. CONCLUSION

In summary, we have experimentally demonstrated the interesting CHB phenomenon in two different propagation schemes of applied laser beams. Four controllable CHBs are observed in the probe absorption spectrum when the coupling (saturating) field co- or counterpropagates with respect

to the probe field. In the reverse case, however, we instead observe three controllable CHBs with the middle one being much deeper. Our experimental results are in good agreement with corresponding numerical simulations (qualitative analysis) in the bare-state (dressed-state) representation. The CHB technique developed here is expected to have potential applications in both classical and quantum optical information storage as well as processing.

ACKNOWLEDGMENT

This work is supported by the National Natural Science Foundation under Grant No. 10334010.

[1] W. R. Bennett, Phys. Rev. **126**, 580 (1962).
[2] W. E. Lamb, Phys. Rev. **134**, A1429 (1964).
[3] A. Renn, U. P. Wild, and A. Rebane, J. Phys. Chem. A **106**, 3045 (2002).
[4] T. Bottger, G. J. Pryde, and R. L. Cone, Opt. Lett. **28**, 200 (2003).
[5] M. Nilsson, L. Rippe, S. Kroll, R. Klieber, and D. Suter, Phys. Rev. B **70**, 214116 (2004).
[6] J. J. Berry, M. J. Stevens, R. P. Mirin, and K. L. Silverman, Appl. Phys. Lett. **88**, 061114 (2006).
[7] S. E. Harris, Phys. Today **50**(7), 36 (1997).
[8] M. Fleischhauer, A. Imamoglu, and J. P. Marangos, Rev. Mod. Phys. **77**, 633 (2005).
[9] S. E. Harris and L. V. Hau, Phys. Rev. Lett. **82**, 4611 (1999).
[10] C. Liu, Z. Dutton, C. H. Behroozi, and L. V. Hau, Nature (London) **409**, 490 (2001).
[11] M. D. Lukin, Rev. Mod. Phys. **75**, 457 (2003).
[12] J. J. Longdell, E. Fraval, M. J. Sellars, and N. B. Manson, Phys. Rev. Lett. **95**, 063601 (2005).
[13] P. Dong and J. Y. Gao, Phys. Lett. A **265**, 52 (2000).
[14] J. H. Wu, X. G. Wei, D. F. Wang, Y. Chen, and J. Y. Gao, J. Opt. B: Quantum Semiclassical Opt. **6**, 54 (2004).
[15] In Ref. [14], numerical simulations are performed for a general Λ-type atomic system. That is, no specific atom is explicitly referred to, so that the wavelength ratio of two possible dipolar transitions can be modified at will.
[16] As to the other two possible schemes of both coupling and saturating beams co- or counterpropagating with the probe, no special experimental phenomena can be found except for a Doppler absorption profile.
[17] All CHBs will become much deeper and clearer if coherence dephasings due to laser linewidths and atomic collisions can be further suppressed.
[18] J. P. Galaup, Opt. Spectrosc. **98**, 722 (2005).
[19] H. Liang, H. Hanzawa, T. Horikawa, and K. Machida, Chem. Lett. **35**, 726 (2006).